Available online at www.sciencedirect.com
SCIENCE DIRECT®
Journal of the European Ceramic Society 24 (2004) 3521–3528
www.elsevier.com/locate/jeurceramsoc

# Preparation and crystallization of glasses in the system tetrasilicic mica-fluorapatite-diopside

D. U. Tulyaganov, S. Agathopoulos, H. R. Fernandes, J. M. Ventura, J. M. F. Ferreira*

*Department of Ceramics and Glass Engineering, University of Aveiro, CICECO, 3810-193 Aveiro, Portugal*

Received 30 September 2003; received in revised form 24 November 2003; accepted 28 November 2003

Available online 13 April 2004

**Abstract**

The production of glasses whose composition ranged between tetrasilicic mica and fluorapatite-diopsite 50/50 (in wt.%) was investigated. Glass-ceramics were obtained by both bulk crystallization and sintering of glass powder compacts. The experimental results showed that increasing amount of apatite and diopsite components in the ternary system until 50% mica content generally caused decrease of melting temperature and increasing stability of glass against spontaneous crystallization during cooling after casting. Liquid immiscibility, whose features depend on the particular glass composition, characterized all the investigated glasses but it was more pronounced in the glasses with higher amount of apatite and diopsite components. The investigated glasses are preferably crystallized in bulk form between 700 and 900 °C, resulting in formation of different combinations between mica, fluorapatite and diopsite, depending on the particular composition. The obtained glass-ceramics exhibited attractive aesthetics, structural integrity and dense structure.
© 2004 Elsevier Ltd. All rights reserved.

*Keywords:* Microstructure-final; Glass; Glass-ceramics; Mica; Apatite

## 1. Introduction

The development and study of new glasses and glass-ceramics for orthopaedic and dental applications have attracted increasing interest in the past decades.[1–7] Biocompatibility (with respect to the absence of toxic effects and potential bioactivity that accelerates healing process) and matching of mechanical properties between materials and living tissues are the two important requirements which anticipate long viability and functionality of a material in the body.[8,9] In the particular case of dental restorations, ceramics should exhibit resistance against dissolution (i.e. chemical stability), proper aesthetic (i.e. shading), and durability (i.e. mechanical strength and wear resistance). The easy use of customised equipments, such as shaping by simple technological methods and firing at relatively low temperatures, is a great challenge in the production of dental ceramics.[10]

Mica glass-ceramics based on the $SiO_2$–MgO–$MgF_2$–$K_2O$ system are commercially available more than 20 years ago. These materials exhibit unique properties, such as remarkable cleavage, flexibility and elasticity, enabling therefore excellent machinability.[11] Nevertheless, production of the well known Dicor™ castable dental glass-ceramics by investing a wax pattern requires expensive apparatus, such as centrifugal casting machines for melting the glass at 1370 °C and a specially designed ceraming furnace for accurate control of crystallization heat treatment at 1070 °C during 6 h.[12] Moreover, the reaction between mica and the surrounding phosphate-bonded investment results in a weak surface layer, whereas surface lamination is strongly demanded. Furthermore, volatilization of fluorine in form of silicon tetra-fluoride during melting and crystallisation of glass is another fundamental problem in this production process.[13–15]

Several investigations have been carried out to eliminate these problems and improve the properties of mica based glass-ceramics. Denry et al.[15] have prepared lithium containing tetrasilicic mica glass-ceramics and found that the presence of lithium shortens crystallization time and decreases crystallization temperature. The optimal crystallization conditions were 30 min of heat treatment at 950 °C, with a heating rate of 12°/min. Henry and Hill found that the substitution of lithia for magnesia in potassium fluorphlogopite can reduce glass transition temperature, increase the aspect ratio

* Corresponding author. Tel.: +351-234-370242; fax: +351-234-425300.
*E-mail address:* jmf@cv.ua.pt (J.M.F. Ferreira).

0955-2219/$ – see front matter © 2004 Elsevier Ltd. All rights reserved.
doi:10.1016/j.jeurceramsoc.2003.11.026

of fluormica crystals and suppress development of cordierite, whose formation opposes good machinability.[13,16] Beyond studies addressed to synthesis of synthetic derivatives of trisilicic and tetrasilicic micas, composite systems such as fluorphlogopite-leucite,[17] fluorphlogopite-apatite,[18–20] calcium mica-apatite, etc.[21] have been also investigated. The well known glass-ceramic Bioverit®-I, which contains muscovite and fluorapatite, has been successfully used in clinical applications for many years since it exhibits both excellent machinability and high bioactivity.[22]

Accordingly, mica-based composites feature great potential for developing new glass-ceramics for biomedical applications. In this work, glasses and glass-ceramics based on the tetrasilicic mica-fluorapatite-diopside [($KMg_{2.5}Si_4O_{10}F_2$)–($Ca_5(PO_4)_3F$)–($CaMgSi_2O_6$)] system were investigated. In particular, the synthesis of five different glasses, whose composition is positioned between mica and fluorapatite-anortite 50/50 (Fig. 1), as well as their crystallization at several temperatures and times are presented (concentration is always quoted in wt.%). For comparison, some compositions that have been already reported in the literature are also marked in Fig. 1. The binary fluorapatite-diopside system has been already investigated in the framework of a thorough study on phase equilibriums taken place in the ternary fluorapatite-anorthite-diopside system.[23] That study has shown that the $Ca_5(PO_4)_3F$–$CaMgSi_2O_6$ binary system has eutectic point at 22.5%/77.5% $Ca_5(PO_4)_3F$/$CaMgSi_2O_6$ and melting point at 1250 °C. Moreover, there is a miscibility gap between 40 and 60% in $Ca_5(PO_4)_3F$ (Fig. 1).

The results of biomineralization capability of the produced materials as well as the in vitro biological testing in cell culture media are beyond the scope of this presentation and will be presented in another article.

## 2. Materials and experimental procedure

The compositions of the batches of the investigated glasses plotted in Fig. 1 are positioned along a straight cross section of the $KMg_{2.5}Si_4O_{10}F_2$–$Ca_5[PO_4]_3F$–$CaMgSi_2O_6$ ternary phase diagram. For simplicity reasons, the composition of tetrasilicic mica is denoted as 1 and the composition 50% fluorapatite/50% diopside as 5. There are three more compositions between them: 2, 3 and 4, containing 75% mica (2) 50% mica (3), and 25% mica (4). Table 1 summarizes the chemical composition of the batches of the investigated glasses.

Powders of technical grade silicon oxide (purity > 99.5%), calcium carbonate (>99.5%), and reagent grade $NH_4H_2PO_4$, $K_2CO_3$, $4MgCO_3{\cdot}Mg(OH)_2{\cdot}5H_2O$, $Na_2CO_3$, $MgF_2$ and $CaF_2$ were used. Homogeneous mixtures of batches (~100 g), obtained by ball milling, were preheated at 900 °C for 1 h and then melted in corundum crucibles at 1350–1500 °C (depending on the composition) for 1 h, in

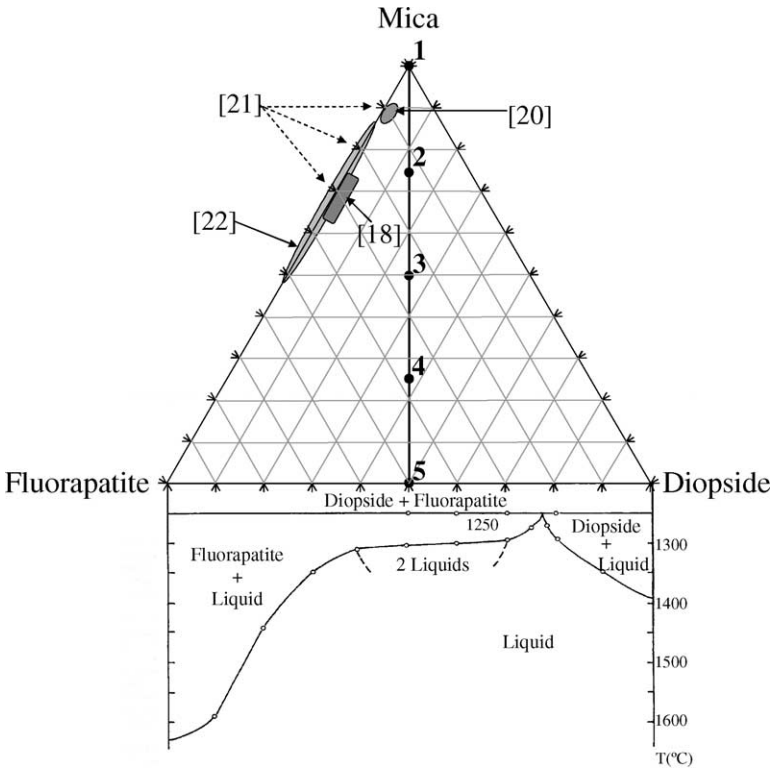


Fig. 1. Composition (in wt.%) of the batches of the investigated glasses 1–5 and details of the apatite-diopsite binary system.[23] (Table 1 shows the oxide composition). Other compositions that have been already reported in the literature are also marked.[18,20–22] Note that in ref. 21 the compositions of glasses are reported in mineral form, while in refs. 18,20,22, in oxides. In the latter case, the showing areas in the diagram were calculated by the authors.

Table 1
Chemical compositions (in wt.%) of the batches of the investigated glasses

| Oxides | Glasses | | | | |
|---|---|---|---|---|---|
| | 1 | 2 | 3 | 4 | 5 |
| $SiO_2$ | 58.59 | 50.88 | 43.17 | 35.46 | 27.75 |
| MgO | 14.73 | 13.37 | 12.01 | 10.66 | 9.30 |
| CaO | – | 9.49 | 18.98 | 28.48 | 37.97 |
| $K_2O$ | 11.48 | 8.61 | 5.74 | 2.87 | – |
| $CaF_2$ | – | 0.97 | 1.93 | 2.90 | 3.87 |
| $MgF_2$ | 15.19 | 11.39 | 7.60 | 3.80 | – |
| $P_2O_5$ | – | 5.28 | 10.56 | 15.83 | 21.11 |

Fig. 1 shows the compositions in mineral form.

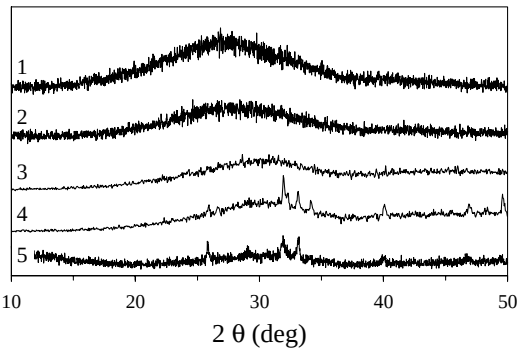


Fig. 2. XRD patterns of the as-cast investigated glasses (after annealing).

air. Glasses in bulk form were produced by casting of melts on preheated bronze moulds and appropriate annealing at temperatures between 550 and 600 °C for 1 h, i.e. close to transformation temperature ($T_g$). Glasses in frit form were also obtained by quenching of melts into cold water.

Bulk crystallization of glass blocks was done in electrical furnace at several temperatures between 700 and 1075 °C with a heating rate of 5°/min. Glass-ceramics were also produced via sintering using glass frit. The frit was dried and then milled in a high-speed porcelain mill to get particle size smaller than 45 μm. Cylindrical pellets (∅ 1 cm) were prepared by uniaxial pressing (200 MPa) and then sintered at several temperatures between 800 and 1250 °C for 1 h and heating rate of 5°/min.

The properties and structural features which can outline the potential of producing these glasses and glass-ceramics were determined using the following techniques. Differential thermal analysis (DTA, Labsys Setaram TG-DTA/DSC, France) of glass powders was carried out in air until 1000 °C with a heating rate of 5°/min. Dilatometry measurements (Bahr Thermo Analyse DIL 801 L, Germany) of glass and glass-ceramic samples were obtained until 900 °C with a heating rate of 3°/min. The crystalline phases formed were detected by X-ray diffraction (XRD, Rigaku Geigerflex D/Mac, C Series, Cu Kα radiation, Japan). The microstructure at polished and then etched surfaces (immersion in 2 vol.% HF solution for 1–5 min) was observed by scanning electron microscopy (SEM, Hitachi S-4100, Japan, 25 kV acceleration voltage). The apparent density of glass and glass-ceramic blocks was measured by Archimedes method (immersion in ethylenoglycol).

## 3. Results and discussion

### 3.1. Formation and microstructure of glasses

The investigated glasses exhibited different behaviour with regards to melting and casting ability. Composition 1 melted at 1420 °C for 1 h was easily cast, forming a transparent glass provided that casting was rapid. In some cases, however, white zones were spontaneously developed in the transparent glass matrix during casting. In compositions 2 and 3, increasing amounts of apatite and diopside apparently caused decrease of melting temperature to 1350–1380 °C and remarkable increase of glass stability against spontaneous crystallization. Composition 2 formed a transparent glass, while composition 3 was solidified into a milky glass. Composition 4 melted at higher temperatures (1430 °C) than compositions 2 and 3, and showed a tendency to form a milky glass after cooling, like composition 3. The melting and easy casting of the batch made of composition 5 required considerably higher temperature (1500 °C).

In glasses 4 and 5, X-ray analysis showed that fluorapatite crystals have been already precipitated during cooling of the melt (Fig. 2). In the case of composition 4, the production of glass without crystalline inclusions was achieved by increasing heating temperature to 1450 °C.

The microstructure of the investigated annealed glasses clearly featured liquid–liquid phase separation (Fig. 3). In the case of glass 1, round particles with a radius 0.3–0.5 μm were embedded in glassy matrix (Fig. 3a). It has been reported that in tetrasilicic mica glasses, droplets enriched in Mg, K and F can precipitate in silicate matrix phase.[24] The microstructure of glass 2 comprises numerous smaller spherical droplets (0.1−0.2 μm) homogeneously distributed in glass matrix (Fig. 3b). Increasing amount of apatite and diopside resulted in more intense phase separation. Thus, in glass 3, there was coexistence of three glassy phases: relatively big spheres (0.10−0.20 μm) and very small droplets (∼10 nm) were dispersed in glass matrix (Fig. 3c). In glass 4, the big spheres have larger dimensions, 0.4−0.5 μm (Fig. 3d). Similar morphology has been reported for glasses which contained both apatite and phlogopite, where large $P_2O_5$-rich spheres and small droplets enriched in Mg, Al, Na(K) and F were embedded in glass silicate matrix.[24] Most likely, the tendency of glasses with relatively high volume fraction of apatite and diopside to favour phase separation as well as the formation of large spherical droplets caused strong opacity effect (light scattering) resulting in the milky appearance of glasses 3 and 4. The composition 5, which belongs to the binary fluorapatite-diopside system, exhibited characteristic phase separation where numerous small droplets (less than 100 nm in size) were homogeneously distributed in glass matrix.[23] It should be noted that the tiny size of these parti-

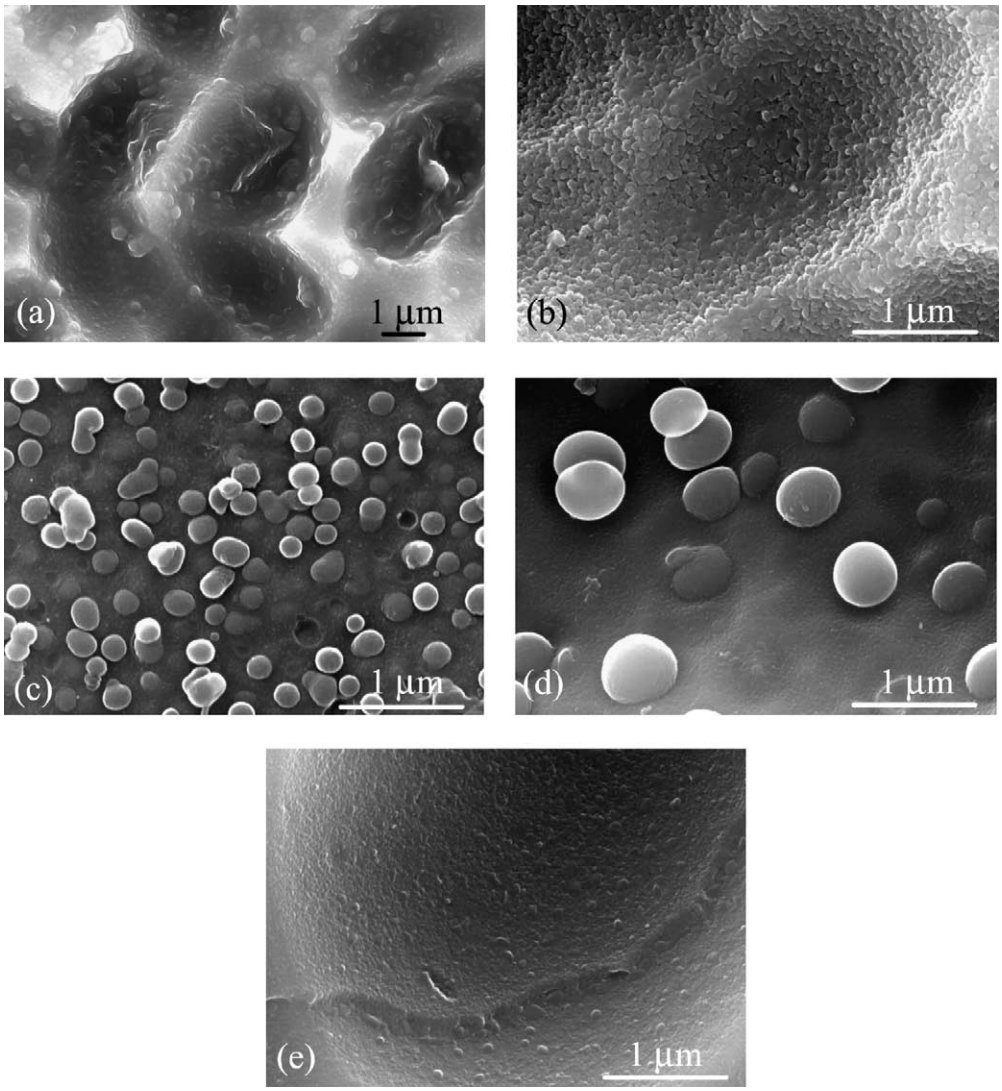


Fig. 3. Microstructure of annealed glasses (a) 1, (b) 2, (c) 3, (d) 4, and (e) 5 (etching with 2 vol.% HF for 1 min).

cles made impossible accurate determination of their chemical composition by EDS analysis.

The temperature dependence of relative expansion ($\Delta l/l_o$) for all the investigated glasses is presented in Fig. 4. The transition temperature ($T_g$) and the dilatometric softening point ($T_s$) of the glasses 1–3 range at 610−630 °C and 650−670 °C, respectively. Increasing apatite and diopside content in glasses 4 and 5 caused increasing of both $T_g$ and $T_s$. From these curves, the values of linear thermal expansion coefficient (CTE) were measured and summarized in Table 2. In general, the glasses with the highest content of apatite and diopside have the highest CTE values.

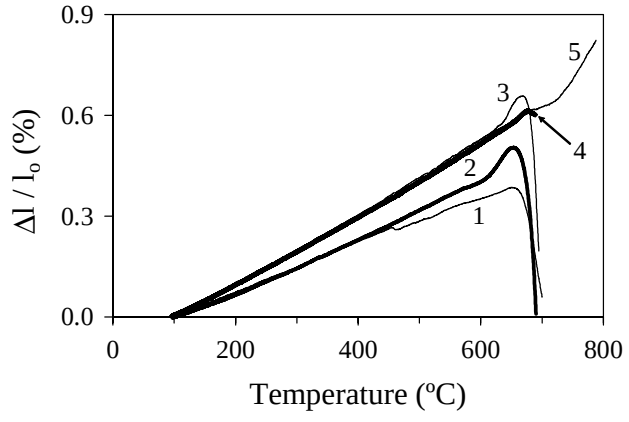


Fig. 4. Relative thermal expansion ($\Delta l/l_o$) of the investigated glasses.

### 3.2. Bulk crystallization

All the investigated glasses featured high capability for bulk crystallization over heating between 700 and 1075 °C. There was also no evidence of formation of pores or voids under observation with optical and electron microscope. The appearance of the block specimens treated at several temperatures is summarized in Table 3. Similarly to Dicor system,[13] in the investigated glass blocks, amorphous phase separation should result in nucleation, which evidently de-

Table 2
Thermal expansion coefficient (CTE) of glasses and glass-ceramics

| Temperature range (°C) | CTE ($\times 10^{-7}$ K$^{-1}$) | | | | |
|---|---|---|---|---|---|
| | 1 | 2 | 3 | 4 | 5 |
| Glasses | | | | | |
| 100–300 | 70.9 | 72.4 | 91.2 | 94.1 | 97.1 |
| 100–600 | 69.5 | 80.6 | 104.0 | 102.0 | 105.0 |
| Glass-ceramics | | | | | |
| 100–600 | 62.8 | 91.4 | 93.4 | 93.9 | 90.6 |
| Preparation parameters | | | | | |
| Temperature (°C) | 1075 | 1000 | 1000 | 1050 | 1000 |
| Soaking time (h) | 5 | 1 | 2 | 1 | 2 |

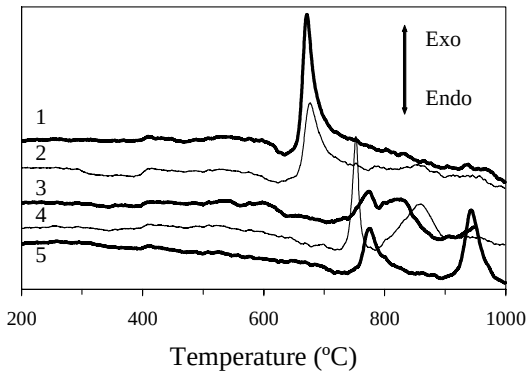


Fig. 5. Differential thermal analysis (DTA) of the investigated glasses.

pends on the content of apatite and diopside in the glass (Fig. 3).

The evolution of phases at different temperatures is thoroughly revealed in Figs. 5 and 6 and summarized in Table 4. A single crystallization peak at 673 °C was observed in composition 1 indicating precipitation of a single crystalline phase from glass reservoir. XRD analysis confirmed that tetra-silicic mica has been already formed at 700 °C. In glass 2, there was a strong exothermic peak at 680 °C and two shallow weak peaks at 754 and 792 °C. The XRD spectra showed that mica was already precipitated at 700 °C while apatite and diopside at 800 °C. The sequence of crystallization changes in composition 3 where precipitation of apatite (exothermic peak at 775 °C) precedes crystallization of diopside and mica (whose both crystallization should result in the shallow exothermic peak between 800 and 840 °C). The composition 4 showed similar behaviour with 3. Apatite (777 °C) and diopside (945 °C) were regularly crystallized in composition 5. Consequently, tetrasilicic mica is crystallized from glass 1 and apatite and diopside from glass 5, while the crystallization of the other intermediate glasses 2–4, resulted in formation of combination between these three phases (mica, apatite and diopside).

Table 4
Evolution of phases in glasses heated at different temperatures for 1 h

| Sample | Phases | | | |
|---|---|---|---|---|
| | 700 °C | 800 °C | 900 °C | 1000 °C |
| 1 | M | M | M | M |
| 2 | M | M + D (+FA*) | M + D + FA | M + D + FA |
| 3 | G | FA + D | M + D + FA | M + D + FA |
| 4 | FA | FA + D | M + D + FA | M + D + FA |
| 5 | FA | FA | FA + D | FA + D |

FA: fluorapatite, D: diopside, M: mica, G: glassy phase. *: traces. See also Figs. 5 and 6.

The degree of crystallization at each temperature can be correlated to the increase of density (Fig. 7). With regards to the different compositions, density regularly increased over increasing amount of apatite and diopsite, except glass-ceramic 5, which has lower density than 4 and even 3 at elevated temperatures. Most probably, composition 5 contains higher amount of glassy phase, evidently indicating a poor crystallization capability. Owning to the fact that the densest glass-ceramics were generally crystallized between 1000 and 1050 °C, prolonged heat treatment was also carried out at 1000 and 1075 °C. Table 5 summarizes the density of the resulting glass-ceramics.

Table 3
Appearance of as-cast annealed glasses and glass-ceramics made via bulk crystallization at several temperatures

| Temperature (°C)/ soaking time (h) | Appearance 1 | Appearance 2 | Appearance 3 | Appearance 4 | Appearance 5 |
|---|---|---|---|---|---|
| | Glass | | | | |
| | Transparent | Transparent | Milk glass | Milk glass | Transparent |
| After heat treatment | | | | | |
| 700 °C/1 h | Transparent | Semi transparent white opaline | Milk glass | Milk glass | Transparent |
| 800 °C/1 h | Semi transparent opaline | White translucent opaline | White opaque | White opaque | Transparent |
| 850 °C/1 h | White translucent opaline | White translucent opaline | White opaque | White opaque | Translucent |
| 900 °C/1 h | White translucent opaque | White translucent opaline | White opaque | White opaque | White translucent opaline |
| 950 °C/1 h | White translucent opaque | White translucent opaline | White opaque | White opaque | White translucent opaline |
| 1000 °C/1 h | White translucent opaque | White translucent opaline | White opaque | White opaque | White translucent opaline |
| 1050 °C/1 h | White translucent opaque | White translucent opaque | White opaque | White opaque | White translucent opaline |
| 1075 °C/5 h | White translucent opaque | Strong deformation | Small deformation | White opaque | White translucent opaline |

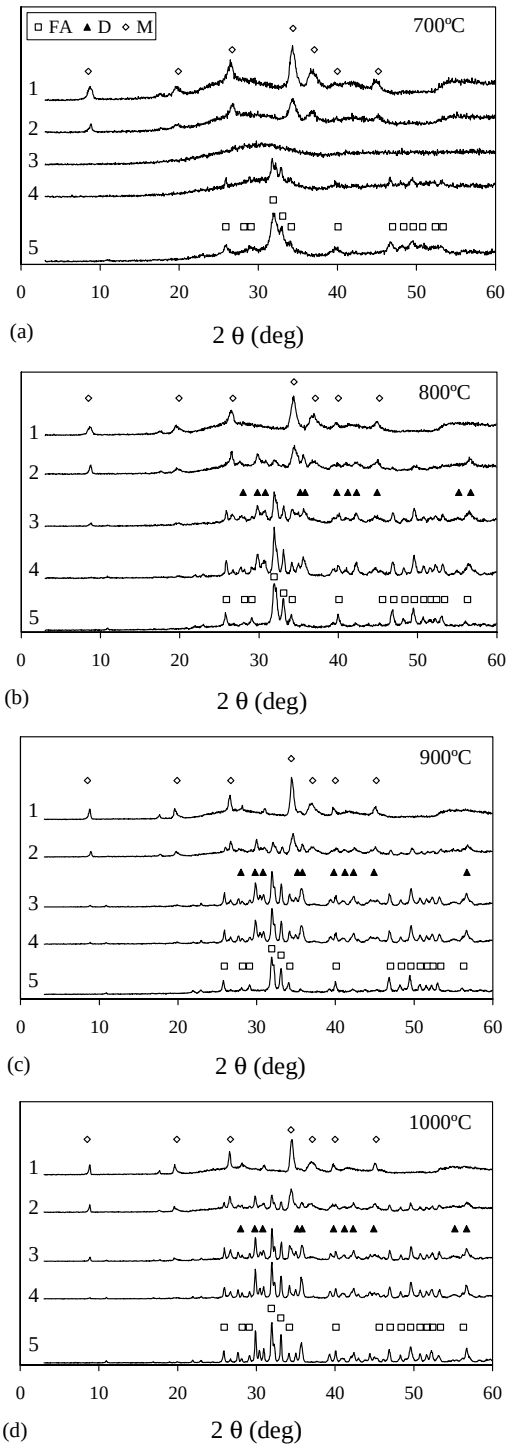


Fig. 6. XRD patterns obtained from glass blocks crystallized at (a) 700 °C, (b) 800 °C, (c) 900 °C and (d) 1000 °C for 1 h. The evolution of the phases is summarized in Table 4. (JCPDS cards: fluorapatite "FA" ($Ca_5(PO_4)_3F$): 15-0876; diopsite "D" ($CaMgSi_2O_6$): 86-0932; potassium magnesium silicate fluoride "M" ($K_{0.88}Mg_{2.5}Si_4O_{10}F_2$): 73-2459).

The microstructure of glass-ceramics crystallized at temperatures, where the highest density values were obtained (Fig. 7 and Table 5), are shown in Fig. 8. Typical "house card" structure[11,25] of randomly oriented interlocked mica crystals (1.5–3.0 μm) was observed in glass-ceramics 1 crystallized at 1075 °C for 5 h (Fig. 8a). Similar configuration of mica crystals (1–2 μm) together with smaller round crystals of apatite (0.2–0.3 μm) were formed after heating of glass 2 at 1000 °C for 1 h (Fig. 8b). Heating of the same glass (2) at higher temperature (1050 °C for 1 h) caused coarsening of structure (Fig. 8c). Evidently, impinging effect of growing mica crystals should have negatively affected densification of the glass-ceramic (decreasing density of glass-ceramic 2 at 1050 °C, Fig. 7). Glass-ceramics 3 crystallized at 1000 °C for 2 h (Fig. 8d) had similar microstructure with 4 crystallized at 1050 °C for 1 h (Fig. 8e). The dense structure comprised interlocked almost spherical (0.2–0.3 μm) and ellipsoid crystals (0.5–1.0 μm), likely nucleated from the separated droplets and observed in the parent glasses (Fig. 3c and d, respectively). Owning to the low intensity of mica peaks in the XRD spectra (Fig. 6d), the crystals observed by SEM should be mostly apatite and diopside. The microstructure of glass-ceramic 5 crystallized at 1000 °C for 2 h (Fig. 8f) is totally different, resembling a monolith formed from relatively big crystals (note that apatite and diopside were identified in XRD) and glassy phase, which seemingly occupies large areas. This finding is in accordance with the aforementioned interpretation of the low density of glass-ceramics 5 crystallized at elevated temperatures (Fig. 7). Similarly to the comment made on glass microstructures, the tiny size of the crystals made impossible an accurate determination of neither their chemical composition nor that one of the glassy matrix by EDS analysis.

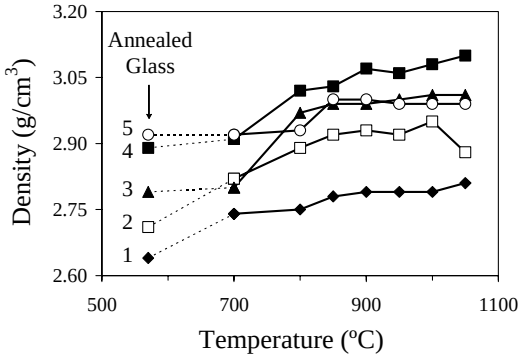


Fig. 7. Dependence of density of glass-ceramics on crystallization temperature, with soaking time of 1 h. (The first values correspond to the density of the as-cast annealed glasses.) See also Table 5.

Table 5
Density of the investigated glass-ceramics crystallized at different conditions

| Temperature (°C)/soaking time (h) | Density (g/cm$^3$) | | | | |
|---|---|---|---|---|---|
| | 1 | 2 | 3 | 4 | 5 |
| 1000/2 | 2.81 | 2.92 | 3.04 | 3.08 | 2.99 |
| 1000/5 | 2.81 | 2.90 | 2.98 | 3.09 | 2.98 |
| 1075/5 | 2.80 | 2.66 | 2.95 | 3.09 | 2.70 |

See also Fig. 7.

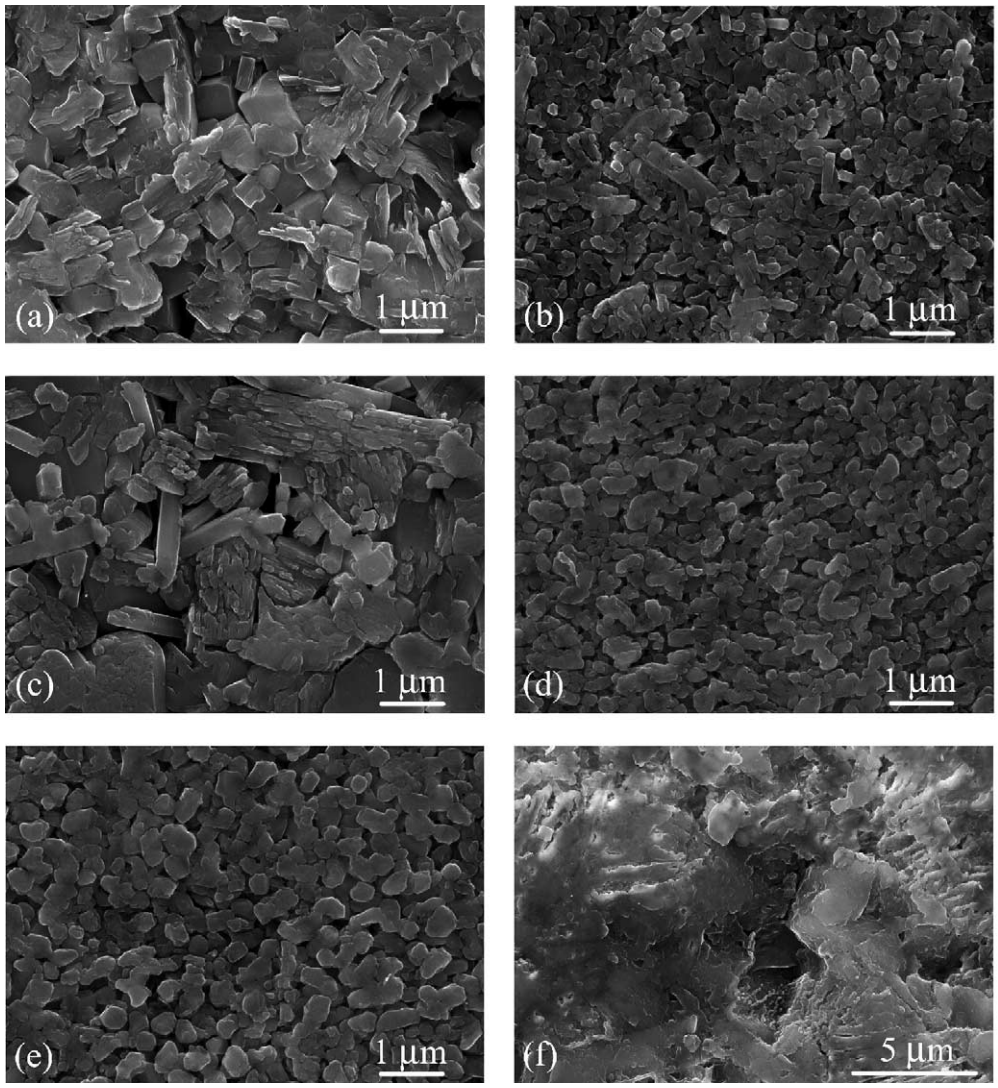


Fig. 8. Microstructure of glass-ceramics (a) 1 (1075 °C, 5 h), (b) 2 (1000 °C, 1 h), (c) 2 (1050 °C, 1 h), (d) 3 (1000 °C, 2 h), (e) 4 (1050 °C, 1 h), and (f) 5 (1000 °C, 2 h) (etching with 2 vol.% HF for 5 min).

The CTE values of the produced glass-ceramics were also measured and the results are summarized in Table 2. With regards to biomedical applications, these values are of special interest in the particular case of potential coating applications where the matching of expansion coefficients between the coating layer and the substrate is of crucial importance.

### 3.3. Crystallization of glass powder

The pellets of glass powder (frit) compacts sintered between 800 and 1250 °C featured poor densification (i.e. negligible increase of density). Among them, the compositions 2–4 exhibited better sintering ability than compositions 1 and 5. Maximum density values were achieved at 1200 °C, i.e. 2.62 g/cm$^3$ for 1, 2.83 g/cm$^3$ for 2, and 3.02 g/cm$^3$ for 3. Heating at 1250 °C caused general decrease of density, while deformation occurred in the samples made of the compositions 2–4.

In the production of glass-ceramics via this method, the desired order of events generally presumes that sintering stage should end before the beginning of intensive crystallization. Then, the resulting glass-ceramic will feature highly dense structure with low porosity. However, the investigated glasses are preferably crystallized in bulk form, where crystalline phases form at temperatures between 700 and 900 °C. Obviously, the formation of crystals causes a shift of sintering to higher temperatures. In the investigated glasses, the maturing range, where sintering and successful densification can safely take place, was very short because it was evidently very close to the liquidus line of the ternary tetrasilicic mica-apatite-diopside system (i.e. characteristic abrupt formation of liquid phase in this temperature region occurred).

## 4. Conclusions

The production of five glasses whose composition ranged between tetrasilicic mica and fluorapatite-diopsite 50/50 (in wt.%) showed the following features:

(a) Increasing amounts of apatite and diopsite components until 50% mica content caused decreasing of melting temperature and increasing stability of glass against spontaneous crystallization during cooling.
(b) All the glasses showed liquid immiscibility, which is more pronounced in the case of higher content of fluorapatite and diopsite components in the ternary system, in terms of the number of the coexisting phases as well as the size of the separated inclusions.
(c) Liquid immiscibility should have caused formation of milky glasses and led crystallization mechanism.
(d) The investigated glasses are preferably crystallized in bulk form between 700 and 900 °C, resulting in formation of different combinations between mica, fluorapatite and diopsite. The ternary glass-ceramics exhibited attractive aesthetics, relatively high thermal expansion ($91 \times 10^{-7}$–$94 \times 10^{-7}\,K^{-1}$) and density ($2.90$–$3.09\,g/cm^3$).

## Acknowledgements

The financial support of CICECO (D.T.) and the Portuguese Foundation of Science and Technology (S.A.) are gratefully acknowledged.

## References

1. Hench, L. L., Bioceramics. *J. Am. Ceram. Soc.* 1998, **81**, 1705–1728.
2. Kokubo, T., Shigematsu, M., Nagashima, Y., Tashiro, M., Nakamura, T., Yamamuro, T. *et al.*, Apatite- and wollastonite-containing glass-ceramics for prosthetic application. *Bull. Inst. Chem. Res.* 1982, **60**, 260–268.
3. Yamamuro, T., A/W glass-ceramic: clinical applications. In *An Introduction to Bioceramics*, ed. L. L. Hench and J. Wilson. World Scientific, Singapore, 1993, pp. 89–103.
4. Kokubo, T., Kim, H. M., Kawashita, M. and Nakamura, T., Novel ceramics for biomedical applications. *J. Aust. Ceram. Soc.* 2000, **36**, 37–46.
5. Vogel, W. and Höland, W., Development of glass-ceramics for medical application. *Angew. Chem. Int. Ed. Engl.* 1987, **26**, 527–544.
6. Höland, W., Schweiger, M. and Rheiberger, V., Nucleation process in glass-ceramics. In *Proceedings of the International Congress on Glass*, Extended Abstracts, *Vol 2*. Edinburgh, Scotland, 1–6 July 2001, pp. 11–12.
7. Karlsson, K. H., Bioactivity of glass and its relation to glass structure. *Glass Phys. Chem.* 1998, **24**, 280–284.
8. Park, J. B., *Biomaterials Science and Engineering*. Plenum Press, New York, 1987.
9. Suchanek, W. and Yoshimura, M., Processing and properties of hydroxyapatite-based biomaterials for use as hard tissue replacement implants. *J. Mater. Res.* 1998, **13**, 94–117.
10. Ironside, J. G. and Swain, M. V., Ceramics in dental restorations: a review and critical issues. *J. Aust. Ceram. Soc.* 1998, **34**, 78–91.
11. Beall, G. N., Glass-ceramics: recent development and applications. *Ceram. Trans.* 1993, **30**, 241–266.
12. Wassell, R. W., Walls, A. W. G. and Steele, J. G., Crowns and extracoronal restorations: materials selection. *Br. Dent. J.* 2002, **192**, 199–211.
13. Henry, J. and Hill, R. G., The influence of lithia content on the properties of fluorphlogopite glass-ceramics. I. Nucleation and crystallization behaviour. *J. Non-Cryst. Sol.* 2003, **319**, 1–12.
14. Wood, D. J., Bubb, N. L., Clifford, A., Hill, R. G. and Knowles, J. C., An investigation into the crystallization of Dicor glass-ceramic. *J. Mater. Sci. Lett.* 1999, **18**, 1001–1002.
15. Denry, I. L., Lejus, A. M., Thery, L. and Masse, M., Preparation and characterization of a new lithium-containing glass-ceramics. *Mater. Res. Bull.* 1999, **34**, 1615–1627.
16. Henry, J. and Hill, R. G., The influence of lithia content on the properties of fluorphlogopite glass-ceramics. II. Microstructure hardness and machinability. *J. Non-Cryst. Sol.* 2003, **319**, 13–30.
17. Ibrahim, D. M. and El-Maliegy, E. A., Mica leucite dental porcelain. *Br. Ceram. Trans.* 2001, **100**, 260–264.
18. Chen, X., Hench, L., Greenspan, D., Zhong, J. and Zhang, X., Investigation on phase separation. *Ceram. Int.* 1998, **24**, 401–410.
19. Yu, B., Liang, K. and Gu, Sh., Effect of the microstructure on the mechanical properties of $CaO$–$P_2O_5$–$SiO_2$–$MgO$–$F^-$ glass ceramics. *Ceram. Int.* 2003, **29**, 695–698.
20. Hamzawy, E. M. A., Crystallization behaviour of fluorphlogopite glass-ceramics. *Ceram. Silikaty* 2001, **45**, 89–96.
21. Taruta, S., Mukoyama, K., Suzuki, S. S., Kitajima, K. and Takusagawa, N., Crystallization process and some properties of calcium mica-apatite glass-ceramics. *J. Non-Cryst. Sol.* 2001, **296**, 201–211.
22. Höland, W. and Vogel, W., Machinable and phosphate glass-ceramics. In *An Introduction to Bioceramics*, eds. L. L. Hench and J. Wilson. World Scientific, Singapore, 1993, pp. 125–137.
23. Tulyaganov, D. U., Phase equilibrium in the fluorapatite-anorthite-dioside system. *J. Am. Ceram. Soc.* 2000, **83**, 3141–3146.
24. Vogel, W., *Chemistry of Glass*. The American Ceramic Society, Westerville, OH, 1985.
25. Höland, W. and Beall, G., *Glass-Ceramic Technology*. The American Ceramic Society, Westerville, OH, 2002.